# Synthesis and Structure of $CrSbSe_3$: A Pseudo-One-Dimensional Ferromagnet

Debra A. Odink, Véronique Carteaux, Christophe Payen, and Guy Ouvrard*

*Laboratoire de Chimie des Solides Institut des Matériaux, UMR 110 CNRS, 2 rue de la Houssinière, 44072 Nantes Cedex 03, France*

*Received June 29, 1992. Revised Manuscript Received December 7, 1992*

Single crystals of $CrSbSe_3$ can be prepared by reaction of the elements in a 1:1:3 ratio at 700 °C. The structure of this compound has been determined using single-crystal X-ray diffraction methods and can be described as pseudo-one-dimensional with double rutile chains of $CrSe_6$ aligned parallel to the crystallographic *b* axis. This compound crystallizes in the Pnma space group with lattice parameters, $a$ = 9.146 (1) Å, $b$ = 3.7851 (7) Å, and $c$ = 13.424 (2) Å. Atomic coordinates were refined to a reliability factor of $R$ = 3.9% ($R_w$ = 2.9%). Magnetic measurements show that $CrSbSe_3$ is ferromagnetic with $T_c$ = 72 K and the primary magnetic exchange is between Cr atoms in the same chain.

## Introduction

Lamellar structures in materials chemistry form a large group of compounds that have been employed as lubricants, catalysts, and most extensively as cathodic materials in energy-storage devices.[1] While much work is yet concerned with more familiar lamellar materials such as transition metal dichalcogenides, graphite, and transition-metal oxides and oxychlorides,[2,3] recent research interests have focused on the development of new lamellar materials that exhibit the desired properties required for intercalation. Several new families of host materials have recently been reported, and these include the transition-metal thiophosphates ($MPS_3$),[4] the layered lanthanide oxychlorides,[5] and the novel transition-metal oxysulfides ($V_2O_4S$).[6] Of these new host systems, the $MPS_3$ phases present very unique structural features as well as interesting physical properties including low-dimensional magnetic behavior,[4] spontaneous magnetization (intercalated $FePS_3$),[7] and transition-metal site rearrangement upon intercalation ($NiPS_3$).[8] Current research interest in this area has shifted to investigating the substitutional capabilities within this structure type. The general theme in these investigations has been the manipulation of properties through electronic modifications in these materials.

The $MPX_3$ compounds can be described as containing $M^{2+}$ cations and $(P_2X_6)^{4-}$ anions in a distorted $CdI_2$ or $CdCl_2$ structure type (or more simply, $M^{2+}$, $P^{4+}$, and $X^{2-}$). Considered in this way, one third of the octahedral metal sites are occupied by a P–P bonded pair and the remaining two thirds by M (detailed structural descriptions of these phases can be found in the literature).[4] It has been observed that only those transition metals with a stable +2 oxidation state form the $MPX_3$ phase (X = S, Se). On the basis of this formalism, one can envision that similar structures may be obtained for transition metals in the +3 oxidation state by the substitution of phosphorous by group IV elements. This has been successful and in addition, $MTX_3$ compounds (where T represents either group IV or group V elements) containing main-group ions for M have also been isolated.[9]

To date, however, no work has been reported on the substitution of larger group V elements (As, Sb, Bi) for phosphorous. Provided the T–T bonded moiety is still present in these compounds (an unlikely result as the size of T increases), materials analogous to the already-mentioned $MPX_3$ compounds could be expected. These compounds would of course show a progressive distortion of the structure with size of the group V element. However, if the T–T bonded species were not formed, new structures may be obtained for transition metals with stable +3 oxidation state. We have been successful in substituting larger group V element for phosphorous in the $MPX_3$ family. This compound, $CrSbSe_3$, can be described as pseudo one-dimensional with $CrSe_6$ double rutile chains aligned parallel to the *b* axis. In this paper we present the crystal structure and static magnetic behavior of $CrSbSe_3$.

## Experimental Section

**Synthesis.** The reaction between chromium (Koch Light, 99.999%), antimony (Johnson-Matthey, Specpure), and selenium (Alfa, 99.999%) in a 1:1:3 molar ratio at 700 °C for 5 days in evacuated quartz ampules yields silver needle crystals of $CrSbSe_3$. The product is air stable. The powder X-ray diffraction pattern of the product shows a small amount of $Sb_2Se_3$. Efforts to improve the yield of $CrSbSe_3$ by reaction at 600 and 800 °C were not successful.

**Characterization.** Quantitative analysis of the elements in the crystals was obtained from a JEOL JSM 35C scanning electron

* To whom correspondence should be addressed.

(1) Whittingham, M. S.; Jacobson, A. Eds.; *Intercalation Chemistry*; Materials Science Series; Academic Press: New York, 1982. Dresselhaus, M. S., Ed.; *Intercalation in Layered Materials*; NATO ASI Series B, Plenum, New York 1986; Physics Vol. 148.

(2) Whittingham, M. S. *Prog. Solid State Chem.* **1985**, *12*, 41. Rouxel, J. in *Chemical Physics of Intercalation*; NATO ASI Series B; Legrand, A. P., Flandrois, S., Eds.; Plenum: New York, 1987; pp 127–147.

(3) *Intercalated Graphite*; Dresselhaus, M. S., Dresselhaus, G., Fischer, J., Moron, M.; Mat. Res. Soc. Proc.; North Holland: New York, 1983, Vol. 20.

(4) Brec, R. *Solid State Ionics* **1986**, *22*, 3–30.

(5) Odink, D. A.; Kang, S.; Kauzlarich, S. M. *Chem. Mater.* **1992**, *4*, 906. Odink, D. A.; Kauzlarich, S. M. *Mol. Cryst. Liq. Cryst.* **1990**, *181*, 325.

(6) Tchangbedji, G.; Odink, D. A.; Ouvrard, G. *J. Power Sources*, in press.

(7) Clement, R.; Lomas, L.; Audiere, J. P. *Chem. Mater.* **1990**, *2*, 641.

(8) Ouvrard, G.; Prouzet, E.; Brec, R.; Benazeth, S.; Dexpert, H. *J. Solid State Chem.* **1990**, *86*, 238–248.

(9) Ouvrard, G.; Sandre, E.; Brec, R. *J. Solid State Chem.* **1988**, *73*, 27–32. Sandre, E.; Carteaux, V.; Ouvrard, G. *C. R. Acad. Sci.* **1992**, *314*, 1151.

0897-4756/93/2805-0237$04.00/0 

**Table I. Observed and Calculated *d* Spacings for $CrSbSe_3$ (Orthorhombic, *a* = 9.146 (1) Å, *b* = 3.7851 (7) Å, *c* = 13.424 (2) Å)**

| *h* | *k* | *l* | $d_{calc}$ | $d_{obs}$ | $I_{obs}$ | $I_{calc}$ |
|---|---|---|---|---|---|---|
| 1 | 0 | 2 | 5.41 | 5.40 (2) | 19 | 22 |
| 2 | 0 | 1 | 4.33 | 4.33 (1) | 8 | 8 |
| 1 | 0 | 3 | 4.019 | 4.020 (8) | 16 | 16 |
| 2 | 0 | 3 | 3.198 | 3.198 (5) | 8 | 8 |
| 1 | 0 | 4 | 3.151 | 3.148 (5) | 5 | 5 |
| 2 | 1 | 0 | 2.916 | 2.915 (4) | 15 | 18 |
| 2 | 1 | 1 | 2.849 | 2.848 (4) | 100 | 100 |
| 2 | 0 | 4 | 2.706 | 2.706 (4) | 54 | 50 |
| 2 | 1 | 2 | 2.674 | 2.675 (4) | 14 | 24 |
| 1 | 0 | 5 | 2.576 | 2.575 (3) | 16 | 16 |
| 2 | 1 | 3 | 2.443 | 2.442 (3) | 5 | 5 |
| 1 | 1 | 4 | 2.422 | 2.421 (3) | 8 | 10 |
| 2 | 0 | 5 | 2.315 | 2.316 (3) | 5 | 7 |
| 4 | 0 | 0 | 2.286 | 2.287 (3) | 4 | 6 |
| 0 | 1 | 5 | 2.190 | 2.190 (2) | 31 | 30 |
| 3 | 1 | 3 | 2.097 | 2.098 (2) | 11 | 11 |
| 4 | 0 | 3 | 2.036 | 2.036 (2) | 5 | 4 |
| 3 | 1 | 4 | 1.938 | 1.939 (2) | 19 | 16 |
| 0 | 2 | 0 | 1.893 | 1.892 (2) | 31 | 23 |
| 4 | 1 | 2 | 1.879 | 1.879 (2) | 26 | 19 |
| 3 | 0 | 6 | 1.804 | 1.804 (2) | 3 | 1 |
| 4 | 1 | 3 | 1.793 | 1.794 (2) | 12 | 12 |
| 4 | 1 | 4 | 1.691 | 1.691 (1) | 4 | 4 |
| 1 | 1 | 7 | 1.682 | 1.682 (1) | 9 | 10 |
| 2 | 2 | 4 | 1.551 | 1.551 (1) | 14 | 15 |
| 3 | 0 | 9 | 1.3398 | 1.3396 (8) | 11 | 7 |
| 8 | 1 | 0 | 1.0944 | 1.0942 (5) | 10 | 23 |

microscopy/EDS system which gave the chemical formula $CrSbSe_3$.[10] A suitable crystal was chosen and mounted into a 0.2-mm glass capillary. Preliminary Bragg and Weissenberg photographs showed an orthorhombic cell with cell parameters (*a*–*c*) 9.195, 13.491, and 3.796 Å. The cell constants were then refined from data collected on an INEL powder X-ray diffractometer (Cu $K\alpha_1$) equipped with a position-sensitive detector, to *a* = 9.146 (1) Å, *b* = 3.7851 (7) Å, *c* = 13.424 (2) Å (silicon used as an internal standard). Table I shows the observed and calculated *d* spacings along with observed and calculated intensities.

The crystal was then transferred to an Enraf-Nonius CAD4 single-crystal diffractometer. Experimental parameters for the data collection and refinement are presented in Table II. The structure was determined via direct methods using the MOLEN structure determination package.[11]

Static magnetic measurements were performed using a Quantum Design SQUID magnetometer. The sample was ground and placed in a gelatin capsule.

Electrical measurements have been performed at room temperature on a thin needle (0.1 × 0.01 × 0.01 $cm^3$), from which a resistivity higher than $10^3$ Ω cm can be deduced. Such nonmetallic behavior is confirmed by the band structure, calculated using the extended Hückel method.[12]

## Results and Discussion

**Structure.** $CrSbSe_3$ crystallizes in the *Pnma* space group (orthorhombic) with cell parameters measured by the diffractometer of *a* = 9.128 Å, *b* = 3.775 Å, *c* = 13.46 Å. These parameters agree with those calculated from powder X-ray diffraction data (see Experimental Section). Atomic coordinates, bond distances and angles are given in Tables III and IV, respectively. The structure can be described as pseudo-one-dimensional with chains of $CrSe_6$ octahedra aligned parallel to the *b* axis. The Cr–Se bond distances observed in these octahedra (2.4–2.6 Å) are comparable to those reported for other Cr–Se compounds.[13] These octahedra are linked together through four common edges and form what is referred to as double rutile chains.[14] Figure 1 shows the double rutile chain as constructed from edge shared octahedra as well as the Cr–Se distances in one octahedron.

The antimony atoms link adjacent chains together to give the pseudo-one-dimensional structure. Each antimony is closely associated with three seleniums on one end of the double rutile chain (Sb–Se2 2.642 (1) Å, 2 bonds, and Sb–Se3 2.665 (2) Å, as shown in Figure 1. Distances observed in $Sb_2Se_3$ are comparable and represent strong bonding interactions.[15] The antimony occupies a trigonal pyramidal position relative to these three seleniums. The pseudo-one-dimensional structure is a result of a weaker bond (3.142 (2) Å) between antimony and Se1 from an adjacent chain. A similar Sb-Se bond has been observed in $Sb_2Se_3$ (3.22 Å). Other atoms are located at distances greater than 3.5 Å from antimony and therefore not

**Table II. Analytical and Crystallographic Data for $CrSbSe_3$**

formula: $CrSbSe_3$ (mol wt 410.63 g/mol)
crystal symmetry: orthorhombic, *Pnma*
cell parameters refined from INEL: *a* = 9.146 (1) Å, *b* = 3.7851 (7) Å, *c* = 13.424 (2) Å
*V* = 462.3 (2) $Å^3$
*Z* = 4
density: 5.90 $g/cm^3$
absorption coefficient: 313.8 $cm^{-1}$

Data Collection
temperature: 293 K
radiation: Mo $K\alpha_{ave}$
monochromator: oriented graphite (002)
scan mode: $\omega/2\theta$
recording angle range: 1.5–35°
scan angle: 0.9 + 0.5 tan θ
values determining scan speed: SigPre = 0.7, σ = 0.03, VPre = 7° $min^{-1}$, $T_{max}$ = 60 s
standard reflections: 0 –6 0, –3 –9 0, 0 –3 –1
period of intensity control: 3600 s
period of orientation control: 300 reflections
abs min 0.522, abs max 1.708, abs ave 0.993

Refinement Conditions
reflections for the refinement of cell dimensions: 22 recorded in the 1/4 space
utilized reflections: 664 with $I > 3\sigma(I)$
refined parameters: 17
reliability factors: $R = \sum|F_o - F_c|/\sum|F_o|$; $R_w = [\sum_w(|F_o| - |F_c|)^2/\sum F^2_o]^{1/2}$

Refinement Results
*R* = 3.9%, $R_w$ = 2.9%
extinction coefficient: $E_c = 4.688 \times 10^{-8}$
difference Fourier maximum peak intensity: 1.9 (2) e/$Å^3$

**Table III. Atomic Coordinates and Thermal Factors for $CrSbSe_3$, Space Group *Pnma*[a]**

| atom | *x*/*a* | *y*/*b* | *z*/*c* | site multiplier | *B* ($Å^2$) |
|---|---|---|---|---|---|
| Sb | 0.9705 (1) | 0.75 | 0.34214 (8) | 1/2 | 1.28 (1) |
| Se1 | 0.9981 (2) | 0.75 | 0.1087 (1) | 1/2 | 0.87 (2) |
| Se2 | 0.7848 (2) | 0.25 | 0.2872 (1) | 1/2 | 1.04 (2) |
| Se3 | 0.8282 (2) | 0.75 | 0.5155 (1) | 1/2 | 0.94 (2) |
| Cr | 0.1549 (3) | 0.25 | 0.0446 (2) | 1/2 | 0.82 (3) |

[a] Anisotropically refined atoms are given in the form of the isotropic equivalent displacement parameter defined as $^4/_3[a^2B(1,1) + b^2B(2,2) + c^2B(3,3) + ab(\cos\gamma)B(1,2) + ac(\cos\beta)B(1,3) + bc(\cos\alpha)B(2,3)]$.

(10) Atom % (calc): 19 (20) Cr, 20 (20) Sb, 61 (60) Se.
(11) MOLEN distributed by Enraf-Nonius, 1990.
(12) Carteaux, V. Thesis, University of Nantes, France, 1992.

(13) For $M_xCrSe_2$, Cr–Se distances are 2.4–2.6 Å, see the following references: Rüdorff, W.; Ruston, W. R.; Scherhaufer, A. *Acta Crystallogr.* **1948**, *1*, 196. Tigchelaar, D.; Haange, R. J.; Weigers, G. A.; van Bruggen, C. F. *Mater. Res. Bull.* **1981**, *16*, 729–739.
(14) Wells, A. F. *Structural Inorganic Chemistry*, 5th ed.; Clarendon: Oxford, 1984; pp 214, 450, 491.
(15) Tideswell, N. W.; Kruse, F. H.; McCullough, J. D. *Acta Crystallogr.* **1957**, *10*, 99.

**Table IV. Relevant Bond Distances (angstroms) and Angles (degrees) in $CrSbSe_3$[a]**

| | | | | | |
|---|---|---|---|---|---|
| Sb | Sb | 3.775 (0) [2] | Se1 | Se1 | 3.775 (0) [2] |
| Sb | Se1 | 3.142 (2) [1] | Se1 | Se2 | 3.618 (2) [2] |
| Sb | Se2 | 2.643 (1) [2] | Se1 | Se2 | 3.516 (2) [2] |
| Sb | Se2 | 3.847 (1) [2] | Se1 | Se3 | 3.741 (2) [2] |
| Sb | Se3 | 2.665 (2) [1] | Se1 | Se3 | 3.443 (2) [1] |
| Sb | Cr | 3.765 (2) [2] | Se1 | Cr | 2.520 (2) [2] |
| | | | Se1 | Cr | 2.486 (3) [1] |
| Se2 | Se2 | 3.775 (0) [2] | Se3 | Se3 | 3.775 (0) [2] |
| Se2 | Se3 | 3.620 (2) [2] | Se3 | Cr | 2.591 (2) [2] |
| Se2 | Se3 | 3.788 (2) [1] | Cr | Cr | 3.775 (2) [2] |
| Se2 | Cr | 2.598 (2) [1] | Cr | Cr | 3.604 (3) [2] |

| | | | | | | | |
|---|---|---|---|---|---|---|---|
| Se2 | Sb | Se2 | 91.18 (4) [1] | Se1 | Cr | Se1 | 96.99 (8) [1] |
| Se2 | Sb | Se3 | 86.01 (4) [2] | Se1 | Cr | Se1 | 87.90 (7) [2] |
| Cr | Se1 | Cr | 96.99 (7) [1] | Se1 | Cr | Se2 | 87.81 (6) [2] |
| Cr | Se1 | Cr | 92.10 (7) [2] | Se1 | Cr | Se3 | 84.69 (3) [2] |
| Sb | Se2 | Sb | 91.18 (5) [1] | Se1 | Cr | Se3 | 176.8 (1) [2] |
| Sb | Se2 | Cr | 92.95 (6) [2] | Se1 | Cr | Se2 | 173.5 (1) [1] |
| Sb | Se3 | Cr | 91.49 (6) [2] | Se1 | Cr | Se3 | 94.91 (7) [2] |
| Cr | Se3 | Cr | 93.51 (7) [1] | Se2 | Cr | Se3 | 89.53 (7) [2] |
| Se3 | Cr | Se3 | 93.51 (8) [1] | | | | |

[a] Numbers in brackets indicate the multiplicity of the distance or angle.

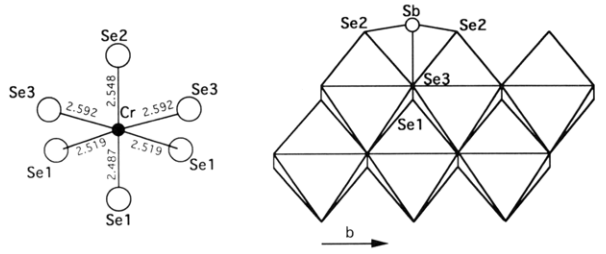


**Figure 1.** Construction of the double rutile chain and $CrSe_6$ octahedron with relevant distances indicated.

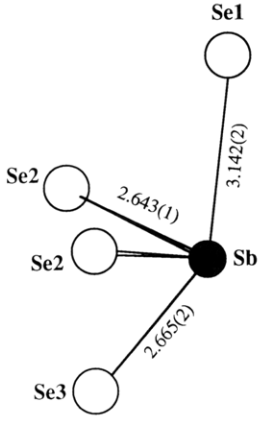


**Figure 2.** Coordination environment of antimony in $CrSbSe_3$.

considered as bonding interactions. These four closest selenium atoms around antimony do not form a regular polyhedral coordination. Figure 2 shows the antimony environment with distances.

In its lower oxidation state III, antimony shares its 5p electrons with elements of comparable electronegativity such as S, Se, or Te, and the $5s^2$ electrons can be considered as a nonbonded pair E. The stereochemical activity of E is related to the loss of sphericity of the $5s^2$ electron distribution.[16] From an antimony coordination point of view, it can be viewed as a distortion effect of a perfect octahedron. The lengthening of some of the Sb–X bonds lowers the coordination number to 5, 4, or 3. The

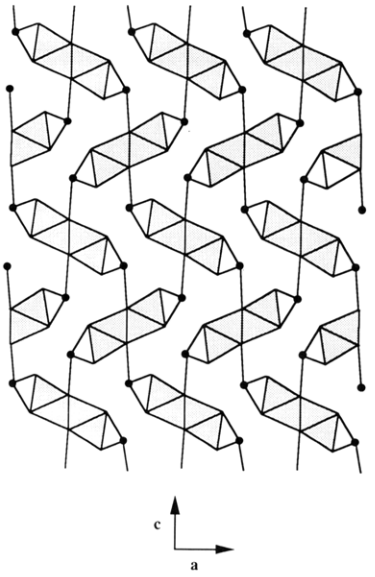


**Figure 3.** Projection view in *ac* plane of $CrSbSe_3$. Polyhedra represent the $CrSe_6$ double rutile chains and shaded circles indicate antimony atoms.

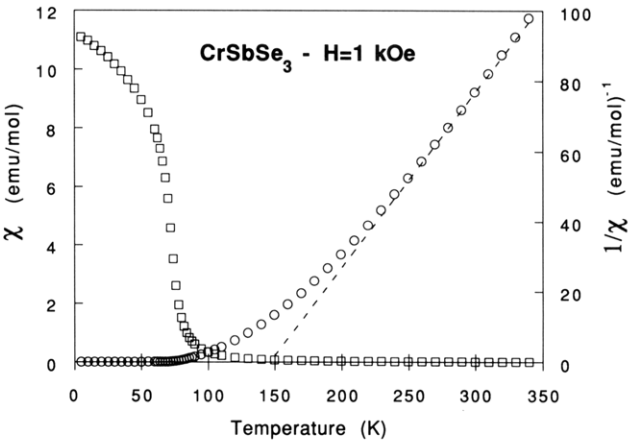


**Figure 4.** Static magnetic susceptibility versus temperature for $CrSbSe_3$ at 1 kOe.

stereochemical activity is then reflected in the coordination number and the discrepancy of Sb–X interatomic distances. The above considerations about Sb–Se distances in $CrSbSe_3$ allow to conclude to a large stereochemical activity of E in this phase. Mössbauer and X-ray absorption spectroscopies experiments are in progress to measure the 5s electron densities which can be related to structural considerations.[17] A projection view of the structure in the ac plane is shown in Figure 3.

**Magnetic Properties.** Figure 4 shows the static magnetic susceptibility measured between 5 and 340 K in an applied field of 1 kOe. The $1/\chi$ plot between 230 and 340 K shows that the magnetic susceptibilty follows the Curie–Weiss law with $\theta = 150$ K and $C = 2$ emu $K^{-1}$ $mol^{-1}$ (effective moment $\mu_{eff} = 4.0\ \mu_B$). The observed Curie constant is close to the spin only value of 1.9 emu $K^{-1}$ $mol^{-1}$ expected for Cr(III) ($\mu_{so} = 3.87\ \mu_B$). These data agree with the expected oxidation degree for chromium of +3 deduced from both the formula unit, $CrSbSe_3$, and the X-ray study. Below 230 K, we observe a deviation from Curie–Weiss behavior.

(16) Olivier-Fourcade, J.; Ibanez, A.; Jumas, J. C.; Maurin, M.; Lefebvre, I.; Lippens, P.; Lannoo, M.; Allan, G. *J. Solid State Chem.* **1990**, *87*, 366.

(17) Olivier-Fourcade, J.; Ibanez, A.; Jumas, J. C.; Dexpert, H.; Blancard, C.; Esteva, J. M.; Karnatak, R. C. *Eur. J. Solid State Inorg. Chem.* **1991**, *28*, 409.

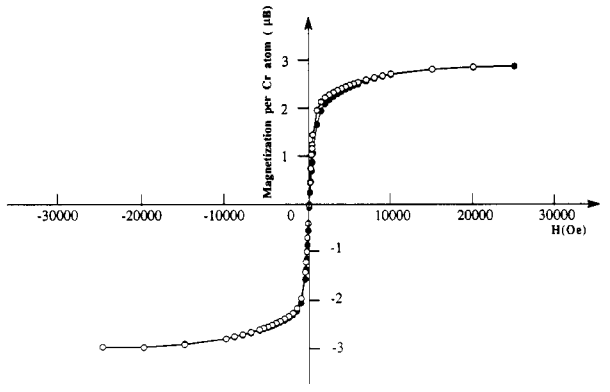


**Figure 5.** Magnetization versus applied field for $CrSbSe_3$ ($T$ = 5 K).

At $T_c$ = 72 K, the onset of long-range ferromagnetic ordering is observed. Magnetization at 5 K up to 25 kOe (shown in Figure 5) confirms the ferromagnetic character of the ordered state. The observed saturation moment of 2.7 $\mu_B$ is slightly lower than the expected value of 3 $\mu_B$ for Cr(III). This difference of the spin-only value is probably due to covalency effects. The hysteresis loop shows the coercitive field ($H_c$) and the remanent magnetization for $CrSbSe_3$ to be very low (Figure 5). The low $H_c$ (10 G) is indicative of a very low concentration of impurity and small internal crystal stress as a result of the slow cooling after the reaction.[18]

It is well known that deviations from Curie–Weiss behavior are a result of magnetic fluctuations occurring above the order–disorder transition temperature ($T_c$).[19] However, short-range order phenomena are expected to extend in a broader temperature range as the dimensionality of the spin lattice decreases.[19] Consequently, we attribute the observed deviation from the Curie–Weiss law to the pseudo-one-dimensional structure inferred from X-ray experiments. Except for the 2D Ising case, an ideal low-dimensional magnet cannot be long-range ordered. Hence, the fact that a 3D transition is observed at a rather high temperature (72 K) shows that coupling between adjacent double rutile chains is not negligible. Nevertheless, the low value of the ratio $T_c/\Theta \approx 0.5$ (which is equal to unity in the molecular field theory) gives convincing evidence for the low dimensionality of the spin network.

Magnetic exchange between adjacent chromiums within the double rutile chains for $CrSbSe_3$ can be correlated to earlier studies on $M_xCrSe_2$ compounds (M = Na, Ag, Hg, Cd).[20] There are two possible magnetic mechanisms for coupling between adjacent Cr atoms. The first is a direct $t_{2g}$–$t_{2g}$ coupling through edge shared octahedra which is antiferromagnetic. This is a result of the half filled $t_{2g}$ states and localization of electrons on the chromium. The other possible magnetic interaction is a superexchange type through selenium orbitals. According to the Goodenough–Kanamori rules,[21] this interaction is ferromagnetic

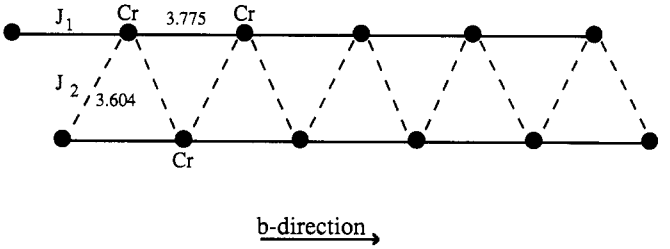


**Figure 6.** Schematic representation of the two magnetic exchange parameters, $J_1$ and $J_2$, in $CrSbSe_3$. Cr–Cr distances are given in angstroms.

**Table V. Magnetic Exchange Parameters for $M_xCrSe_2$ and $CrSbSe_3$ ($J$ Values Are Given for a Spin Hamiltonian $H = -2JS_1S_2$)**

| compound | $d$ (Å) | $\theta$ | $J$/k (K) |
|---|---|---|---|
| $AgCrSe_2$ | 3.68 | 92.9 | 4 |
| $NaCrSe_2$ | 3.73 | 93.5 | 8 |
| $HgCr_2Se_4$ | 3.80 | 97.0 | 16 |
| $CdCr_2Se_4$ | 3.80 | 97.0 | 14 |
| $CrSbSe_3$ $J_1$ | 3.775 | 93.5, 97.0 | |
| $CrSbSe_3$ $J_2$ | 3.604 | 92.1 | |

provided the Cr–Se–Cr angle is close to 90°. Whether the compound exhibits ferromagnetic or antiferromagnetic interactions depends on geometric factors such as $d_{Cr-Cr}$ and the angle Cr–Se–Cr.[20] All the $M_xCrSe_2$ compounds are ferromagnetic and therefore the $d_{Cr-Cr}$ distances are too high for direct $t_{2g}$–$t_{2g}$ antiferromagnetic coupling (Table V). In $CrSbSe_3$, the Cr–Se–Cr angles between shared octahedra in the same rutile chain are 97.04° and 93.49° (corresponding to Cr–Se1–Cr and Cr–Se3–Cr, respectively) and the Cr–Cr distance is 3.775 Å. These values for shared octahedra between rutile chains are 92.09° (Cr–Se1–Cr) and 3.604 Å (Cr–Cr distance). Since there are two types of Cr–Cr distances in $CrSbSe_3$, we can identify two types of interactions designated $J_1$ and $J_2$, which correspond to coupling within the same rutile chain and coupling between chains, respectively. There are schematically represented in Figure 6. To our knowledge no prediction is available for deducing exchange values from susceptibility data in the case of a Heisenberg ladder system. To estimate $J_1$ and $J_2$, we compare the observed values of $d_{Cr-Cr}$, and Cr–Se–Cr angles for the $M_xCrSe_2$ compounds and for $CrSbSe_3$. According to Table V, the $J_1$ coupling must be ferromagnetic and of the order of $J_1 \approx 10$ K (for a spin Hamiltonian $H = -2JS_1S_2$). The $J_2$ value must be lower than $J_1$ as a result of the shorter Cr–Cr distance. On the basis of these comparisons, we conclude that the primary magnetic exchange is between Cr atoms within a single rutile chain. A weaker interaction ($J_2$) is present between chains. This latter interaction is ferromagnetic since an antiferromagnetic $J_2$ should lead to an antiferromagnetic 3D ordering at least up to spin-flop critical field. Indeed, no field-induced transition could be detected in the magnetization versus applied field curve shown in Figure 5.

**Supplementary Material Available:** Listings of $h$, $k$, $l$, $F_o$, $F_c$, $\sigma/F$, and anisotropic thermal parameters (10 pages); list of structure factor amplitudes (9 pages). Ordering information is given on any current masthead page.

(18) Chikazumi, S. *Physics of Magnetism*; Wiley: New York, 1964; p 119.

(19) Domb, C. Statistical Mechanics of Critical Behavior in Magnetic Systems. In *Magnetism*; Rado, G., Suhl, H., Eds.; Academic Press: New York 1965; Vol. IIA.

(20) Colombet, P. Thesis, University of Nantes, France, 1982. Colombet, P.; Danot, M. *J. Solid State Chem.* **1983**, *45*, 311.

(21) Goodenough, J. B. *Magnetism and the Chemical Bond*; Wiley: New York, 1986.